Effect of hydrogen concentration on the surface oxidation of Ni-base alloys in simulated PWR primary water

Yun Soo Lim[*], Dong Jin Kim, Sung Woo Kim, Seong Sik Hwang, Hong Pyo Kim, Min Jae Choi
Materials Safety Technology Development Division/Korea Atomic Energy Research Institute
989-111 Daedeok-daero, Yuseong-gu, Daejeon 34057, Korea
[*]*Corresponding author: yslim@kaeri.re.kr*

1. Introduction

Primary water stress corrosion cracking (PWSCC) of Ni-base Alloy 600 has been a major concern in the primary side of pressurized water reactors (PWRs) [1]. In response to the cracking problems associated with Alloy 600, another solid-solution strengthened Ni-base alloy, Alloy 690, has become the common replacement material in PWR service. Alloy 690 is more resistant to PWSCC than Alloy 600. Dissolved hydrogen is also known to have significant effects on the cracking behavior of Ni-base alloys. Hydrogen is normally added at levels of 25 - 50 cm^3 H_2/kg H_2O to primary water. The PWSCC susceptibilities of Alloy 600 and its weld metals are known to peak near the Ni/NiO transition, and the location of the Ni/NiO transition has been shown to vary with temperature, from 25 cm^3 H_2/kg H_2O at 360 °C to 4 cm^3 H_2/kg H_2O at 288 °C [2].

The aim of the present study was to characterize the internal and IG oxidation phenomena depending on the hydrogen concentration to obtain clear insight into the role of dissolved hydrogen on the different resistance to PWSCC and the cracking behavior of Alloys 600 and 690 when exposed to PWR primary water. After the test, the microchemical changes near the surface and around the grain boundaries due to oxygen diffusion were precisely characterized using various types of microscopic equipment, in this case, scanning electron microscopy (SEM), transmission electron microscopy (TEM), high-resolution TEM (HRTEM) imaging, and fine-probe chemical analysis using energy dispersive X-ray spectroscopy (EDS) in the scanning TEM (STEM) mode. Finally, possible correlations between the internal and IG oxidation and the dissolved hydrogen are discussed on the basis of the observed results

2. Methods and Results

2.1 Materials

A mill-annealed Alloy 600 round bar with an outside diameter of 120 mm was used in this study. The Alloy 600 round bar was finally heat-treated at 950 °C for 3 h and then quenched with water. A forged round bar of Alloy 690 with an outside diameter of 196 mm was also used. The Alloy 690 round bar was finally solution-annealed and then quenched with water. Alloys 600 and 690 used in this study were archive materials for CRDM penetration nozzles for use in a PWR. Detailed information on the microstructure and cracking behavior of the test alloys are described in the literature [3].

2.2 Oxidation Test

Coupons (10 × 10 × 2 mm^3) cut from the round bar were prepared by grinding with SiC paper to a 2000 mesh and subsequently polishing with alumina powders down to 0.3 μm. The simulated PWR water was prepared prior to the test in a storage tank. 1200 ppm B (by weight) of H_3BO_3 and 2 ppm Li (by weight) of Li(OH) were added to pure water. After the removal of the dissolved oxygen by purging with nitrogen gas, hydrogen was added to the simulated PWR primary water. The oxygen concentration was maintained at less than 5 ppb during the test. A 316L stainless steel autoclave with a volume of 3.8 liters was used in a recirculating mode. The specimens were exposed to simulated primary water at hydrogen concentrations of 5, 30 and 50 cm^3 H_2/kg H_2O for a period of 3600 hrs. The test temperature was 325 °C. The combinations of the temperature and the hydrogen concentration used for the present study correspond to the conditions where Ni is in the oxidized state (5 cm^3 H_2/kg H_2O) and Ni is in the metallic state (30 and 50 cm^3 H_2/kg H_2O) [2]. The conductivity, dissolved oxygen concentration, pH, and hydrogen concentration were continuously monitored at room temperature.

2.3 Surface Oxidation Results of Pure Ni

Fig. 1 shows the results of X-ray diffraction (XRD) measurements conducted using pure Ni coupons tested at 325 °C for a period of 3600 hrs to investigate the oxidation behavior of pure Ni. As expected, only X-ray peaks originating from metallic Ni were observed when the hydrogen concentration was 50 cm^3 H_2/kg H_2O, where Ni was in a metallic state [2]. On the other hand, X-ray peaks from NiO emerged when the hydrogen concentration was 5 cm^3 H_2/kg H_2O, where Ni was in an oxidized state [2]. The spinel peaks, identified as $(Ni,Fe)_3O_4$ from EDS measurement, evolved on all of the oxidized Ni specimens as shown in the figure. It appears that the $(Ni,Fe)_3O_4$ spinel oxides were caused by the Ni and Fe ions in the test solution dissolved from the stainless steel components of the test loop containing the autoclave.

When the hydrogen concentration was 50 cm^3 H_2/kg H_2O, faceted oxides identified as $(Ni,Fe)_3O_4$ spinel were

found to randomly distribute on the surface with a variety of sizes. On the other hand, when the hydrogen concentration was 5 cm^3 H_2/kg H_2O, two types of oxides emerged. First, most of the oxides on the surface had pyramidal shapes and they were identified as NiO from Fig. 1. NiO oxides form in this case since the Ni specimen is in an oxidation state at this hydrogen concentration. Another type of oxide was found over the NiO pyramidal oxides, and was identified as $(Ni,Fe)_3O_4$.
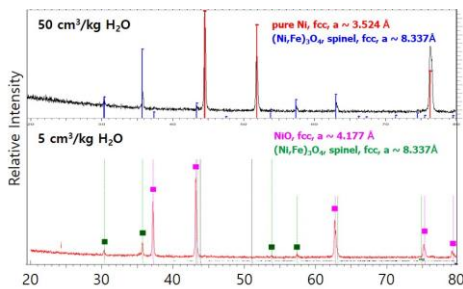

Fig. 1 Results of XRD measurements of pure Ni at hydrogen concentrations of 50 and 5 cm^3 H_2/kg H_2O tested at 325 °C for a period of 3600 hrs.

2.4 Surface Oxidation Results of Alloy 600

The electron microscopic results of Alloys 600 and 690 obtained at the hydrogen concentration of 50 cm^3 H_2/kg H_2O were similar to those at the hydrogen concentration of 30 cm^3 H_2/kg H_2O, respectively. Therefore, results obtained at the hydrogen concentrations of 5 and 30 cm^3 H_2/kg H_2O will be presented in this study.

Fig. 2 was obtained from Alloy 600 at a hydrogen concentration of 30 and 5 cm^3 H_2/kg H_2O tested at 325 °C for a period of 3600 hrs, respectively, presenting a STEM image and EDS spectrum images of O, Cr, Fe, and Ni obtained using the Kα1 lines. A grain boundary is visible in the STEM image. In the O spectrum image, a continuous thin Cr-rich oxide layer appears to emerge. The faceted oxides over the surface grain boundary were identified as (Ni,Fe) spinel. The most intriguing feature in Fig. 2 is that oxygen diffused down along the grain boundary, causing the grain boundary to be oxidized irrespective of the hydrogen concentration.

On the oxidized grain boundary, Cr was enriched. However, Fe and Ni were depleted in the oxidized grain boundary (Fe and Ni spectrum images) compared to the average concentration of the matrix. This indicates that Cr oxide formed in the oxidized grain boundary. Ni was enriched inside the oxidized grain boundary near the surface in the case of Fig. 2(a), which was obtained at the hydrogen concentration of 30 cm^3 H_2/kg H_2O. The formation of Ni-enriched regions is very common during the IG oxidation process of Alloy 600 in primary water whenever oxygen penetrates the metal and Cr is internally oxidized to form an oxide [4]. This behavior of Ni is thought to be mainly attributable to Ni being in

a metallic state at this hydrogen concentration. The noticeable difference in IG oxidation between Fig. (a) and (b) is that, while Ni was enriched in the oxidized grain boundary when Ni was in a reduced state at a hydrogen concentration of 30 cm^3 H_2/kg H_2O, Ni reacted with diffusing oxygen, resulting in the formation of Ni-rich oxides in the oxidized grain boundary when Ni was in an oxidized state at a hydrogen concentration of 5 cm^3 H_2/kg H_2O.
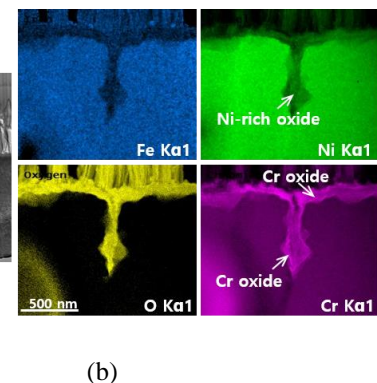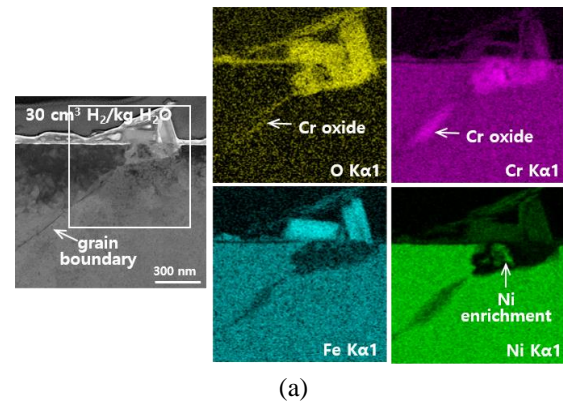

(a)

(b)

Fig. 2 STEM image and EDS spectrum images of O, Cr, Fe, and Ni in Alloy 600 at hydrogen concentrations of (a) 30 cm^3 and (b) 5 cm^3 H_2/kg H_2O, tested at 325 °C for 3600 hrs.

2.5 Surface Oxidation Results of Alloy 690

Fig. 3 shows a STEM image and EDS spectrum images of O, Cr, Fe and Ni around the surface obtained from Alloy 690 at a hydrogen concentration of 30 and 5 cm^3 H_2/kg H_2O, respectively, tested at 325 °C for a period of 3600 hrs. The surface oxidation layers were much thicker than those of Alloy 600 under the same experimental conditions. The most noticeable feature in this figure is that there is no oxygen diffusion along a grain boundary which indicates that IG oxidation did not occur in Alloy 690 irrespective of the hydrogen concentration, in contrast with Alloy 600. From these results, it can be confirmed that the internal and IG oxidation phenomena of Alloy 690 were quite different from those of Alloy 600. The main reason for these differences is thought to be the different chemical compositions, especially the different Cr contents in

these two alloy groups. Ni nodules are visible on the surface in Fig. 3(a), which is similar to the Ni enrichment in the oxidized grain boundary of Fig. 2(a).
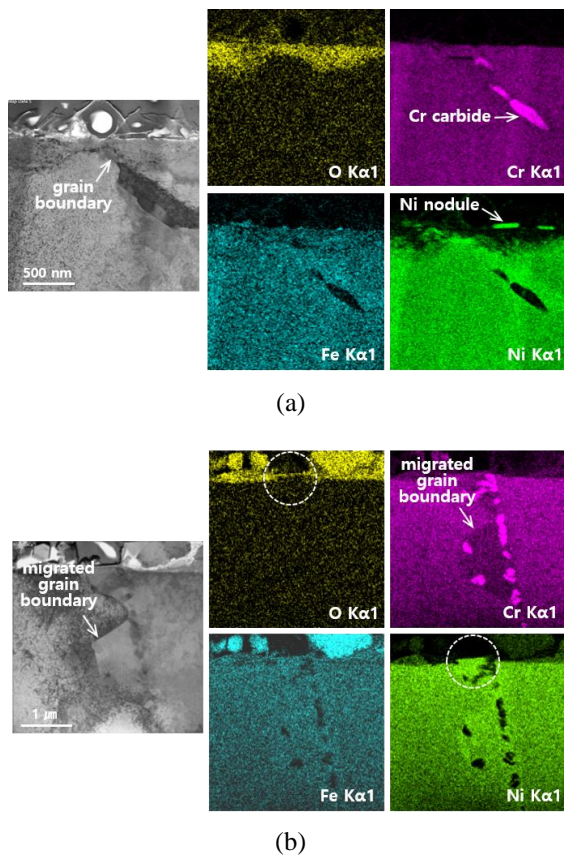

(a)

(b)

Fig. 3 STEM image and EDS spectrum images of O, Cr, Fe, and Ni in Alloy 690 at hydrogen concentrations of (a) 30 cm^3 and (b) 5 cm^3 H_2/kg H_2O, tested at 325 °C for 3600 hrs.

The intriguing features in Fig. 3(b) are that diffusion induced grain boundary migration (DIGM) occurred, and the oxidation layer along the surface swept by DIGM was considerably thin compared to the surrounding layer. Interestingly, there is a Ni-rich region on the swept grain boundary. Recently, DIGM in Ni-base alloys during exposure to simulated PWR primary water or hydrogenated steam has been reported as a commonly occurring process [5], and DIGM has been an attractive research subject in terms of IG oxidation and cracking owing to the accompanying Cr depletion.

3. Conclusions

From the XRD measurements, it was found that Ni was in a reduction state when the hydrogen concentration was 50 cm^3 H_2/kg H_2O, whereas pyramidal oxides identified as NiO emerged on the surface when the hydrogen concentration was 5 cm^3 H_2/kg H_2O at which Ni was in an oxidized state. It was revealed from a TEM examination that surface grain boundaries were oxidized in Alloy 600 within a range of hydrogen concentration between 5 and 30 cm^3 H_2/kg

H_2O. There was Ni enrichment in the oxidized regions of Alloy 600 when the hydrogen concentration was 30 cm^3 H_2/kg H_2O, whereas Ni-rich oxides emerged in the oxidized regions when the hydrogen concentration was 5 cm^3 H_2/kg H_2O. This indicates that the behavior of Ni in Alloy 600 considerably changes depending on the hydrogen concentration. On the other hand, IG oxidation did not occur in Alloy 690 within a range of hydrogen concentration between 5 and 30 cm^3 H_2/kg H_2O. Ni nodules emerged on the surface when the hydrogen concentration was 30 cm^3 H_2/kg H_2O. Therefore, it appears that the formation of Ni nodules or Ni enrichment is common in Ni-base alloys when Ni is in a reduction state. DIGM commonly occurred in Alloy 690 irrespective of the hydrogen concentration. All the above different oxidation phenomena observed in Alloys 600 and 690 depending on the hydrogen concentration are believed to significantly affect their resistance to PWSCC.

Acknowledgements

REFERENCES

[1] W. Bamford, and J. Hall, A review of Alloy 600 cracking in operating nuclear plants: historical experience and future trends, Proc. of the 11th Int. Conf. on Environmental Degradation of Materials in Nuclear Power Systems-Water Reactor, p. 1071, 2003.

[2] S.A. Attanasio and D.S. Morton, Measurement of the Nickel/Nickel Oxide Transition in Ni-Cr-Fe Alloys and Updated Data and Correlations to Quantify the Effect of Aqueous Hydrogen on Primary Water SCC, Proc. of the 11th Int. Conf. on Environmental Degradation of Materials in Nuclear Power Systems-Water Reactor, p. 143, 2003.

[3] Y.S. Lim, D.J. Kim, S.W. Kim and H.P. Kim, Crack growth and cracking behavior of Alloy 600/182 and Alloy 690/152 welds in simulated PWR primary water, Nucl. Eng. Tech., Vol. 51, p. 228, 2019.

[4] Y.S. Lim, S.W. Kim, S.S. Hwang, H.P. Kim and C. Jang, Intergranular oxidation of Ni-based Alloy 690 in a simulated PWR primary water environment, Corros. Sci., Vol. 108, p. 125, 2016.

[5] W. Kuang, M. Song and G.S. Was, Insights into the stress corrosion cracking of solution annealed alloy 690 in simulated pressurized water reactor primary water under dynamic straining, Acta Mater., Vol. 151, p. 321, 2018.